

Normal growth of *Arabidopsis* requires cytosolic invertase but not sucrose synthase

D. H. Paul Barratt^a, Paul Derbyshire^a, Kim Findlay^a, Marilyn Pike^a, Nikolaus Wellner^b, John Lunn^c, Regina Feil^c, Clare Simpson^a, Andrew J. Maule^a, and Alison M. Smith^{a,1}

^aJohn Innes Centre and ^bInstitute of Food Research, Norwich Research Park, Norwich NR4 7UH, United Kingdom; and ^cMax Planck Institute for Molecular Plant Physiology, Wissenschaftspark Golm, Am Mühlenberg 1, 14476 Potsdam-Golm, Germany

Edited by Maarten J. Chrispeels, University of California at San Diego, La Jolla, CA, and approved April 10, 2009 (received for review January 21, 2009)

The entry of carbon from sucrose into cellular metabolism in plants can potentially be catalyzed by either sucrose synthase (SUS) or invertase (INV). These 2 routes have different implications for cellular metabolism in general and for the production of key metabolites, including the cell-wall precursor UDPglucose. To examine the importance of these 2 routes of sucrose catabolism in *Arabidopsis thaliana* (L.), we generated mutant plants that lack 4 of the 6 isoforms of SUS. These mutants (*sus1/sus2/sus3/sus4* mutants) lack SUS activity in all cell types except the phloem. Surprisingly, the mutant plants are normal with respect to starch and sugar content, seed weight and lipid content, cellulose content, and cell-wall structure. Plants lacking the remaining 2 isoforms of SUS (*sus5/sus6* mutants), which are expressed specifically in the phloem, have reduced amounts of callose in the sieve plates of the sieve elements. To discover whether sucrose catabolism in *Arabidopsis* requires INVs rather than SUSs, we further generated plants deficient in 2 closely related isoforms of neutral INV predicted to be the main cytosolic forms in the root (*cin1/cin2* mutants). The mutant plants have severely reduced growth rates. We discuss the implications of these findings for our understanding of carbon supply to the nonphotosynthetic cells of plants.

Most plant cells receive essentially all of their carbon as sucrose. Sucrose catabolism in plants is one of the largest metabolic fluxes on the planet, second only to fluxes in primary carbon assimilation. Only 2 enzymes can catalyze sucrose catabolism under physiological conditions: sucrose synthase (SUS) and invertase (INV); thus, most plant biomass is derived via 1 of these 2 routes. However, despite their central role in carbon partitioning and biomass accumulation, the precise roles and relative importance of these enzymes remain largely unknown.

SUS and INV both occur as multiple, distinct isoforms. INV catalyzes the effectively irreversible hydrolysis of sucrose to glucose and fructose. Isoforms in the cell wall and vacuole (acid INV) differ in structure from those predicted to be in the cytosol, mitochondria and plastids (neutral/alkaline INV). SUS catalyzes the reversible conversion of sucrose to fructose and UDPglucose; SUS isoforms are believed to be cytosolic.

Several lines of evidence indicate a predominant role for SUS in the entry of carbon into metabolism in nonphotosynthetic cells. Individual isoforms are needed for normal development in some plant organs, including potato tuber, pea and maize seed, tomato fruit, and cotton fibers (1–5). SUS is held to be important in determining sink strength, and in phloem loading (1, 6, 7). It is also proposed to have specific roles in cellulose synthesis, and in starch synthesis in leaves. In the widely cited model for cellulose synthesis, the substrate UDPglucose is channeled to the cellulose synthase complex in the plasma membrane via a SUS associated with the inner face of the complex (8, 9). Consistent with this idea, some SUS activity is associated with the plasma membrane (10–12). Leaf starch synthesis is generally believed to occur via a pathway in which the substrate ADPglucose is generated inside the chloroplast, without involvement of SUS. However, a recent alternative proposal is that ADPglucose is generated via SUS from sucrose in the cytosol, then imported

into the chloroplast (13). Evidence for this pathway includes parallel alterations in starch levels in leaves of transgenic potato plants in which SUS activity has been altered (14). If correct, this proposal gives SUS a central role in photosynthetic carbon assimilation and partitioning.

Most of the roles proposed for INVs are specific to particular developmental stages. Vacuolar INV is involved in mobilization of vacuolar sucrose in sucrose-storing organs (15, 16). It is required for normal root elongation in *Arabidopsis*, probably through its impact on vacuolar osmotic potential and, thus, on water uptake (17). Cell-wall INV activity is high after wounding and pathogen attack (18, 19), and in early seed development (20), and is required for normal kernel development in maize (21) and pollen tube extension (22). The functions of neutral INV are not known, but loss of 1 of the 6 isoforms in rice (*OsCYT-INV1*), or 1 of the 7 in *Lotus japonicus* (*LjINV1*), strongly affects plant growth and development (23, 41). Loss of 1 of the 9 isoforms in *Arabidopsis* (*CINV1* or *CYT-INV1*) has much less pronounced effects. It reduces primary root extension by $\approx 30\%$ and can reduce leaf and silique expansion (24, 25).

The route of sucrose catabolism has important implications for energy conservation and carbon allocation in nonphotosynthetic cells. Conversion of sucrose to hexose phosphates via SUS uses only half the ATP needed for conversion via INV. The reversibility of the reactions of the SUS route means flux via this route is sensitive to hexose phosphate levels and, thus, to demand for glycolytic intermediates (26, 27). The requirement for PP_i (as a substrate for UDPglucose pyrophosphorylase) links sucrose catabolism via SUS to other PP_i -requiring processes, including flux over the reversible glycolytic enzyme PP_i -dependent fructose 6-phosphate phosphotransferase. In contrast, the INV-catalyzed reaction is effectively irreversible, and INV isoforms have no reported properties that would allow coordination of sucrose catabolism with carbon demand in nonphotosynthetic cells.

Despite the accepted importance of SUS, we recently showed that none of the 6 isoforms in *Arabidopsis* is individually required for normal growth and reproduction, neither are any of the 3 pairs of most closely related isoforms (*SUS1/SUS4*, *SUS2/SUS3*, and *SUS5/SUS6*) (28). Thus, there must either be a high level of redundancy within the SUS family in *Arabidopsis*, or INV isoforms must be able to compensate for loss of SUS in this species. To explore the implications of this finding, we have generated a quadruple mutant (the *sus1/sus2/sus3/sus4* mutant) that has no detectable soluble or membrane-bound SUS activity. Remarkably, the mutant is normal with respect to growth and development, metabolite levels, seed composition, and the com-

Author contributions: D.H.P.B. and A.M.S. designed research; D.H.P.B., P.D., K.F., M.P., R.F., and C.S. performed research; D.H.P.B., P.D., N.W., J.L., and A.J.M. analyzed data; and A.M.S. wrote the paper.

The authors declare no conflict of interest.

This article is a PNAS Direct Submission.

¹To whom correspondence should be addressed. E-mail: alison.smith@bbsrc.ac.uk.

This article contains supporting information online at www.pnas.org/cgi/content/full/0900689106/DCSupplemental.

position of cell walls. In marked contrast, loss of 2 of the 9 isoforms of neutral INV (the *cinv1/cinv2* mutant) results in severe inhibition of growth. We discuss the implications of these results for understanding of sucrose catabolism in the nonphotosynthetic cells of plants.

Results

Location of SUS Isoforms SUS5 and SUS6. We were previously unable to detect SUS5 or SUS6 proteins in soluble and membrane fractions of *Arabidopsis* plants (28). Surprisingly, both were present in insoluble (mainly cell-wall) material from roots and hypocotyls, and SUS6 was present in this material from stems (Fig. 1A). Neither protein was detected in insoluble material from plants of a double mutant lacking both SUS5 and SUS6 (the *sus5/sus6* mutant) (28). SUS activity in insoluble material from roots and stems was reduced by $\approx 65\%$ in *sus5/sus6* mutant plants (Table 1).

Isoforms SUS1, SUS2, SUS3, and SUS4 were very largely soluble. The insoluble material contained a small fraction of the SUS1 protein (this fact may account for the SUS activity in insoluble material from the *sus5/sus6* mutant), but SUS2, SUS3, and SUS4 were not detectable (Fig. S1). Soluble activity in *sus5/sus6* mutant plants was the same as or greater than that in WT plants (Table 1), indicating that SUS5 and SUS6 do not contribute to soluble activity (the soluble fraction contains both free and membrane-associated SUS activity).

Tissue prints showed that SUS5 and SUS6 proteins were present specifically in the phloem region of the hypocotyl. SUS6 was also detected in this region in stems. No immunoreactive material was present in the *sus5/sus6* mutant (Fig. 1B). Consistent with a phloem location for SUS6, we showed previously that expression of a GUS reporter gene driven by the *SUS6* promoter occurred only in specific cell files within the stele of the root (28). In *in situ* hybridization experiments on roots, *SUS6* transcript was detected only in the protophloem cells (Fig. 1C and D), from which the phloem sieve elements arise. To investigate possible roles of SUS5 and SUS6, we examined sections of stems that were chemically fixed immediately after excision. An electron-translucent layer lining the pores of sieve plates was consistently thinner in the *sus5/sus6* mutant than in WT plants (Fig. S2A and B). ImmunoGold labeling with an anticalllose antibody confirmed that this layer contains callose (Fig. S2C). In contrast, callose synthesis after wounding and callose associated with plasmodesmata in leaves appeared to be the same in WT and mutant plants (Fig. S3). Together, these results suggest that SUS5 and SUS6 are confined to sieve elements where they have a specific function in callose synthesis. Thus, a *sus1/sus2/sus3/sus4* mutant would be expected to lack SUS activity in all cell types except sieve elements.

Phenotype of the *sus1/sus2/sus3/sus4* Mutant. We selected a *sus1/sus2/sus3/sus4* mutant (the quadruple mutant) and confirmed that it lacked all 4 SUS proteins (Fig. S4). As expected, SUS5 and SUS6 proteins were in the same locations in quadruple mutant and WT plants (Fig. 1). SUS activity in the soluble fraction of roots and stems was below the level of detection ($<2\%$ WT levels; Table 1). Thus, the remaining SUS activity in the quadruple mutant is highly likely to be located exclusively in cell walls of phloem sieve elements.

Quadruple mutant plants were not visibly different from WT plants when grown in well-drained compost under natural daylight or short days (Fig. S5). WT and mutant plants were the same with respect to carbohydrate levels in roots, stems, siliques and leaves, seed weight, seed oil content (Table 1, Table S1, and Table S2), callose in sieve plates, and callose in plasmodesmata and after wounding (Fig. S2 and S3). The only exception was a 50% higher starch content in siliques of mutant plants (Table S1 and Table S2).

We used several methods to examine cellulose location and content in the quadruple mutant. There was no difference

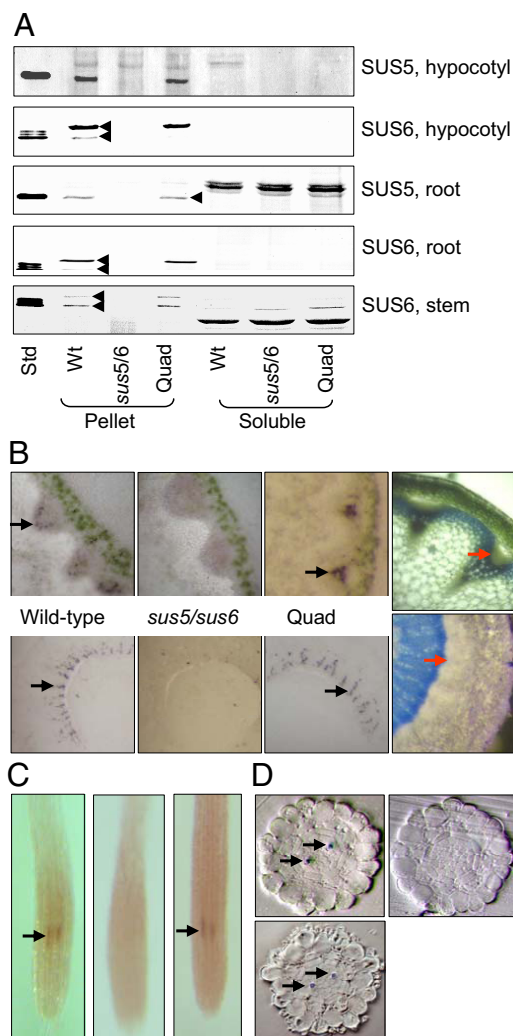


Fig. 1. Location of SUS6 transcript and protein in WT and quadruple mutant plants. Pictures are representative of multiple plants for each genotype and treatment. (A) Blots of hypocotyl extracts (from 11-week-old plants grown in short days), stems (as in Table 1), whole root systems (from 5-week-old plants grown in an inert medium), and purified SUS proteins (28) (Std, SUS5 protein for SUS5 antiserum; SUS6 protein for SUS6 antiserum) were probed with SUS5 or SUS6 antiserum (28). In each panel, lanes are from the same gel and blot. Equal fractions of soluble and pellet material were loaded. Note that bands recognized by the SUS5 antiserum in root soluble fractions are not SUS5 protein. They migrate more slowly than authentic SUS5 (arrowed), and are present in the *sus5/sus6* mutant. The SUS6 antiserum recognizes 2 bands in extracts (arrowed in WT). Both are missing in the *sus5/sus6* mutant, so both are probably SUS6 protein. (B) Tissue prints of stem (Upper) and hypocotyl (Lower) sections probed with SUS6 antiserum. (Left to Right) WT, *sus5/sus6* mutant, *sus1/sus2/sus3/sus4* (Quad) mutant, and a stem section stained with toluidine blue. Black arrows show typical antiserum reactions; red arrows show the equivalent region on the section. (C) Location of *SUS6* transcript in roots by whole-mount *in situ* RNA hybridization. Fixed and cleared roots of 4-day-old seedlings were treated with RNA probes for *SUS6*. (Left) WT with *SUS6* antisense probe; (Center) WT with *SUS6* sense probe; (Right) *sus1/sus2/sus3/sus4* mutant with *SUS6* antisense probe. The appearance of *sus6* mutant roots with *SUS6* antisense probe was the same as WT roots with *SUS6* sense probe. Arrows show RNA hybridization. Root diameter is $\approx 130 \mu\text{m}$. (D) Location of SUS transcript in root sections. Roots as in C were embedded and sectioned at the level at which RNA hybridization was observed. Arrows show hybridization. (Upper Left and Right) Sections of WT roots with *SUS6* antisense probe and *SUS6* sense probe respectively; (Lower Left) a *sus1/sus2/sus3/sus4* mutant root with *SUS6* antisense probe.

between WT and quadruple mutant plants in the appearance of walls of mesophyll and stem xylem cells (Fig. 2A and B), indicating that primary and secondary cell walls are not seriously

Table 1. SUS activity, metabolite contents, and seed weight of WT and mutant plants

Genotype	Sucrose synthase activity, nmol min ⁻¹ g ⁻¹ fresh weight							
	Roots				Stems			
	Soluble		Pellet		Soluble		Pellet	
WT	49.8 ± 3.2		5.3 ± 0.1		27.5 ± 6.6		1.8 ± 0.2	
<i>sus5/sus6</i>	49.8 ± 4.9		1.9 ± 0.5		41.6 ± 6.2		0.6 ± 0.5	
<i>sus1/sus2/sus3/sus4</i>	0.1 ± 0.1		3.4 ± 0.4		0.4 ± 0.3		1.6 ± 0.1	
Genotype	Carbohydrate content, μmol g ⁻¹ fresh weight							
	Leaves				Roots			
	End of day		End of night		End of day		End of night	
	WT	Quad	WT	Quad	WT	Quad	WT	Quad
Glucose	0.59 ± 0.09 (7)	0.64 ± 0.10 (7)	0.22 ± 0.02 (7)	0.14 ± 0.02 (7)	1.5 ± 0.2 (7)	1.9 ± 0.2 (7)	0.48 ± 0.05 (6)	0.58 ± 0.06 (5)
Fructose	0.15 ± 0.03 (6)	0.17 ± 0.02 (6)	0.041 ± 0.012 (6)	0.025 ± 0.004 (5)	0.094 ± 0.006 (6)	1.05 ± 0.07 (6)	0.25 ± 0.04 (6)	0.31 ± 0.03 (6)
Sucrose	1.01 ± 0.19 (7)	1.07 ± 0.19 (7)	0.35 ± 0.04 (7)	0.45 ± 0.03 (7)	1.95 ± 0.22 (7)	2.18 ± 0.34 (7)	0.76 ± 0.10 (6)	0.57 ± 0.08 (6)
Starch	31.5 ± 1.3 (7)	31.4 ± 1.9 (5)	2.4 ± 0.3 (7)	2.6 ± 0.3 (7)	0.20 ± 0.02 (7)	0.21 ± 0.02 (7)	0.18 ± 0.02 (6)	0.15 ± 0.01 (6)
Genotype	Seed weight, mg							Percentage oil
WT	0.0165 ± 0.0007							33.62 ± 1.99
<i>sus1/sus2/sus3/sus4</i>	0.0171 ± 0.0013							33.45 ± 1.38

SUS activity, metabolite contents, seed weight, and lipid content of WT and mutant plants. Roots were from 4- or 5-week-old plants grown in an inert medium. Stems were 4-cm sections from the base of the primary inflorescence of 6-week-old plants grown in compost. Samples from the end of the day and the end of the night were a whole rosette (leaf) or a whole root system (root). Quad, *sus1/sus2/sus3/sus4*. Sus activities are means ± SD from 3 plants; metabolite values are means ± SD from the number of samples shown in parentheses; seed weights are means ± SD from 6 samples from 2 independent pools, each from 5 plants; lipid values are means ± SD from 6 independent pools, each from 5 plants.

disrupted. Mutants deficient in secondary cell-wall synthesis have a collapsed xylem phenotype (29). FTIR microspectroscopy on root cell-wall preparations revealed no major differences in the carbohydrate region of the spectrum between quadruple mutant and WT seedling roots (Fig. 2C; Fig. S6). Scanning FTIR array microscopy of stem sections revealed no differences at a wavelength at which the cell-wall IR spectrum is dominated by cellulose (Fig. 2D; Fig. S6). There was no difference in cellulose content between quadruple mutant and WT stems (42.4 ± 3.3 and 44.6 ± 4.5% of dry weight, respectively; means ± SD from 5 samples; dry weights 6 to 9 mg). We also found no differences between *sus5/sus6* and WT plants with respect to any of the above analyses (cellulose content 42.1 ± 4.3%; Fig. S6).

To examine further the capacity for sucrose catabolism in the quadruple mutant, we analyzed the expression of *INV* genes and the levels of hexose phosphates, UDPglucose, and a range of other primary metabolites. We found no differences between WT and quadruple mutant plants in these respects (Fig. S7, Table S1, and Table S2).

Phenotype of the Neutral INV Mutant *cinv1/cinv2*. The data above showed that *Arabidopsis* plants lacking SUS in all cell types except sieve elements can grow and reproduce normally, without increased expression of INV genes or major perturbations of pool sizes of hexose phosphates and UDPglucose. Thus, it appeared that INV could substitute completely for SUS in sucrose catabolism in *Arabidopsis*, and indeed, that INV rather than SUS might be the dominant route for sucrose catabolism in WT plants. To test this idea, we selected a mutant lacking 2 isoforms of cytosolic INV [CINV1 (24), also called CYT-INV1 (25), encoded at At1g35580; CINV2 encoded at At4g09510]. These isoforms are the 2 most highly expressed neutral/alkaline INV predicted to be located in the cytosol of root cells (<https://www.geneinvestigator.ethz.ch/gv/index.jsp>) (30): the cytosol is the likely location for enzymes important in the entry of carbon from sucrose into cellular metabolism. Mutations in *CINV1* are already known to have a relatively mild effect on *Arabidopsis* growth (24, 25). *CINV1* and *CINV2* are both closely related to a single isoform shown by mutational analysis to be essential for normal growth and development of *L. japonicus* plants (41). We

established that the best available T-DNA insertion line for *CINV2* (Sail518_D02, designated *cinv2*) has only 10% of WT *CINV2* transcript levels in its roots (Fig. S8).

The single mutants *cinv1* and *cinv2* appeared identical to WT plants on soil under our growth conditions. The *cinv1/cinv2* plants flowered and set seed when grown on soil, but were much smaller in all respects than WT plants at maturity (Fig. 3A; Fig. S8). Seedlings of *cinv1/cinv2* had relatively normal shoot growth, but drastically reduced root growth on solid medium without sugar. Whereas primary root extension over 7 days of growth was 60% of the WT value in *cinv1* (24, 25), and 120% of the WT value in *cinv2*, it was only 17% of the WT value in *cinv1/cinv2* [lengths: WT, 5.18 ± 0.16 cm (31); *cinv1*, 3.14 ± 0.11 cm (24); *cinv2*, 5.86 ± 0.14 cm (45); *cinv1/cinv2*, 0.88 ± 0.01 cm (55); mean ± SE, *n* in parentheses; Fig. 3].

Cells in the root expansion zone of *cinv1/cinv2* mutants were enlarged and had a greater tendency to collapse during manipulation than those of WT and single-mutant plants. Abnormal cell divisions occurred in the stele, endodermis, and cortex (Fig. 3). Growth on glucose restored root extension in double mutants to approximately half of WT (Fig. S8). Neutral INV activity in roots was ≈40% lower in double mutant than in WT seedlings (WT, 50.8 ± 2.3; double mutant, 30.5 ± 0.7 nmol min⁻¹ mg⁻¹ protein; mean ± SD, *n* = 3).

Discussion

Our findings have important implications for understanding of plant primary metabolism. It has generally been assumed that SUS is more important than INV in catalyzing the entry of carbon into metabolism in many plant cells. As described above, this route requires less ATP, and allows for feedback regulation of sucrose catabolism, and reductions in SUS in organs of crop plants often have obvious, deleterious effects. However, our results show that soluble SUS is not required for normal growth in *Arabidopsis* under our experimental conditions, whereas cytosolic INV is indispensable.

The requirement for SUS in some tubers, seeds, and fruits of crop plants may reflect the dense and/or bulky nature of these organs, which results in low internal oxygen levels (32) and, thus, reduced ATP supply. Low oxygen levels promote patterns of metabolism that conserve energy, including reliance on SUS

The seedling phenotype of the *cinv1/cinv2* mutant is consistent with general carbon starvation brought about by reduced capacity for sucrose catabolism in root cells. Evidence includes the extreme reduction in root growth, the loss of starch from the root cap (Fig. 3), and the enlargement and tendency to collapse of several cell types. The roots resemble those of mutants defective in cell-wall biosynthesis (35, 36), except that the phenotypes of cell-wall mutants are stronger at high sugar concentrations (37), whereas the phenotype of *cinv1/cinv2* shows the opposite effect. We suggest that cell expansion in roots of *cinv1/cinv2* is abnormal because of a lack of substrate for cell-wall synthesis, rather than a defect in a specific pathway of cell-wall synthesis. The strong promotion of root extension by exogenous glucose also indicates that the phenotype is in part due to carbon starvation.

Caution must be exercised in further interpretation of the strong phenotype of the double *cinv* mutant. The stunted growth may reflect a direct requirement for cytosolic INV in many organs, but it might also be a consequence of a strong inhibition of root growth alone, or of other pleiotropic effects on gene expression and on sugar signaling pathways (as suggested for the *cinv1* mutant) (24). The fact that neutral INV activity is reduced by only 40% in the double mutant is also difficult to interpret. The residual activity may be due to other cytosolic isoforms and/or the isoforms of unknown function located in organelles. We found that loss of *CINV1* expression increases *CINV2* transcript levels (Fig. S8.4); thus, there may be pleiotropic effects on INV activity in the *cinv1/cinv2* mutant.

Together with recent reports for rice (23) and *Lotus* (41), our results show that cytosolic INV is essential for normal plant growth and development. Little is known about this class of enzymes. It is not clear whether they have regulatory properties that would allow flux of carbon out of sucrose via this route to be coordinated with the metabolic demands of the cell, or why SUS cannot compensate for loss of cytosolic INV isoforms. It is interesting to note that AtCINV1 interacts in yeast 2-hybrid experiments with the phosphatidylinositol monophosphate 5-kinase AtPIP5K9, and is coimmunoprecipitated with PIP5K9 from extracts of transgenic plants overexpressing both proteins (24). PIP5K9 is a component of phosphatidylinositol signaling pathways that are necessary for normal root growth. These observations suggest that cytosolic INV may be a target for signaling pathways that coordinate carbohydrate availability with growth and development in nonphotosynthetic organs.

Methods

Plant Material. The *sus* mutant lines were as in ref. 28. The quadruple mutant was created by crossing *sus1/sus4* with *sus2/sus3*. For the *cinv1* mutant (24), absence of *CINV1* transcript was confirmed by RT-PCR.

Unless otherwise stated, plants were grown in compost at 20 °C with 12-h light, 12-h dark, 150–200 μmol quanta $\text{PAR m}^{-2} \text{s}^{-1}$, and 75% relative humidity. Roots of mature plants were harvested from a 1:1 mixture of sand and Terragreen (Oil-Dri) with a slow-release fertilizer. Hypocotyls were harvested after 11 weeks growth in compost at 22 °C with 9-h light, 15-h dark, 95 μmol quanta $\text{m}^{-2} \text{s}^{-1}$, and 65% relative humidity. For seedling roots, seeds were surface sterilized (70% vol/vol aq. ethanol 5 min, \approx 1% vol/vol Na hypochlorite 10 min), rinsed with water, then sown on plates of solid medium (Phytigel, Sigma; 5 g l^{-1} plus inorganic nutrients; see ref. 38) with or without 1% (wt/vol) glucose. After 3 days at 4 °C, plates were placed vertically at 22 °C with 6-h dark, 18-h light at 85 μmol quanta $\text{PAR m}^{-2} \text{s}^{-1}$.

Starch, Metabolite, and Oil Measurements. For starch and metabolite measurements, samples were transferred to liquid nitrogen immediately after cutting. Roots were rapidly rinsed and blotted before freezing. For starch, sugars, hexose

phosphates, and UDPglucose, frozen samples were extracted in 0.7 M perchloric acid, and metabolites assayed enzymatically (34). The UDPglucose assay contained UDPglucose pyrophosphorylase, phosphoglucomutase and NAD-glucose 6-phosphate dehydrogenase. For other metabolites, extraction was in chloroform-methanol and analysis by LC-MS/MS (39). Oil content of mature seeds was measured by NMR spectroscopy (28). Cellulose was assayed chemically on tissue samples powdered in liquid nitrogen before extraction (29).

Immunoblotting, Enzyme Assays, and Tissue Printing. Frozen tissue was powdered then extracted at 4 °C in either 50 mM Na-Hepes (pH 7.5), 5 mM MgCl_2 , 1 mM EDTA, 5 mM DTT, and 10 mL L^{-1} protease inhibitor mixture (Sigma) (for SUS assays), or 50 mM Bis-Tris (pH 7.0), 5 mM ascorbic acid, 5 mM DTT, 2 mM EDTA, 1 mM EGTA, 50 mM NaCl, 10 mL L^{-1} protease inhibitor mixture, and 10 mL L^{-1} phosphatase inhibitor mixture 1 (Sigma) (for immunoblotting). The homogenate was subjected to centrifugation for 10 min at 10,000 $\times g$ and 4 °C. The supernatant is referred to as the soluble fraction. The pellet was washed twice by resuspension in extraction medium using a glass homogenizer, followed by centrifugation, then resuspended either in extraction medium (for assays) or in SDS sample buffer (for SDS/PAGE). The soluble fraction was precipitated with 10% (wt/vol) trichloroacetic acid, then solubilized in SDS sample buffer. SDS/PAGE, immunoblotting, and assays were as described (28). Tissue prints were made by gently pressing cut stems or hypocotyls onto nitrocellulose membrane, then developing as for immunoblotting.

In Situ Hybridization. A DNA template for the last exon of *SUS6* was generated from full-length cDNA by PCR by using the following primers:

5'- AAGAAAGTGACAATCCCGGAAGATAAACCTC-3'

5'- CCTCGATCCAAGGTCAAACCTTTTAAATCTC-3'

T3 (sense) and T7 (antisense) promoter sequences were incorporated by PCR

(5' - AATTAACCCTCACTAAAGGGAAGAAAGTGACAATC-3';

5' - TAATACGACTCACTATAGGGCTCGATCCAAGGTC-3').

PCR-product purification was carried out by using a QIAquick PCR purification kit (QIAGEN). DIG-labeling of the PCR product was done by using the Riboprobe in vitro Transcription System (Promega). Whole mount in situ hybridization was done on 4-day-old seedlings (40).

Microscopy. For light microscopy. Stem sections (30 μm) were cut on a vibratome and stained with 0.02% (wt/vol) toluidine blue O. For root transverse sections (Fig. 3 C and D), roots were cut into 2.5% (vol/vol) glutaraldehyde in 0.05 M Na cacodylate, pH 7.3, vacuum infiltrated and left overnight in fresh fixative. Samples were washed in 0.05 M Na cacodylate, postfixed in 1% (wt/vol) OsO_4 in 0.05 M Na cacodylate for 1 h, washed in distilled water, and dehydrated through an alcohol series. Dehydrated samples were infiltrated with LR White resin by successive changes of resin/ethanol mixes over 5 days at room temperature, then transferred to fresh resin. The resin was polymerized at 60 °C for 16 h. Sections (0.5 μm) were dried onto glass slides and stained with 0.5% (wt/vol) toluidine blue O in 0.5% (wt/vol) borax. For root longitudinal sections (Fig. 3 E and F), roots were fixed overnight in 4% paraformaldehyde at 4 °C, then subjected to a modified pseudoSchiff propidium iodide staining (31). Samples were viewed with a confocal microscope at excitation wavelength 488 nm.

Scanning Electron Microscopy. Samples were mounted on an aluminum stub by using O.C.T. compound (BDH), plunged into liquid nitrogen slush, then transferred onto the cryostage of an ALTO 2500 cryo-transfer system (Gatan) attached to a Zeiss Supra 55 VP FEG scanning electron microscope. After fracturing at -100 °C, samples were sputter-coated with platinum (90 s at 10 mA, <-110 °C), then imaged at 3 kV on the cryo-stage in the main chamber of the microscope at ≈-130 °C.

FTIR Analyses. Cell walls from primary roots were prepared and analyzed as previously (35). Details of FTIR techniques are provided in Fig. S6.

ACKNOWLEDGMENTS. We thank Trevor Wang and Tracey Welham (John Innes Centre) for suggesting selection of the *cinv1/cinv2* mutant and other valuable discussions; Keith Roberts and Irmi Horst (John Innes Centre), Nick Kruger (University of Oxford, Oxford), and Bob Furbank (Commonwealth Scientific and Industrial Research Organisation, Canberra, Australia) for advice and discussions; Grant Calder and Sue Bunnell (John Innes Centre) for expert assistance with microscopy; and Alexander Graf (John Innes Centre) for help with qRT-PCR experiments. This work was supported by a core strategic grant from the Biotechnology and Biological Sciences Research Council to the John Innes Centre.

1. Zrenner R, Salanoubat M, Willmitzer L, Sonnwald U (1995) Evidence of the crucial role of sucrose synthase for sink strength using transgenic potato plants (*Solanum tuberosum* L.). *Plant J* 7:97–107.

2. D'Aoust MA, Yelle S, Nguyen-Quoc B (1999) Antisense inhibition of tomato fruit sucrose synthase decreases fruit setting and the sucrose unloading capacity of young fruit. *Plant Cell* 11:2407–2418.

